Dynamical universality classes of vapor deposition models with evaporation

S. H. Yook and Yup Kim*
Department of Physics and Research Institute for Basic Sciences, Kyung-Hee University, Seoul 130-701, Korea
(Received 7 April 1999)

Growth models for vapor depositions in which evaporation and deposition can occur, both at a randomly chosen column and at its nearest neighbor columns (NNCs), are studied by Monte Carlo simulations. The growth processes in these models are determined by comparing local chemical potentials of the chosen column and its NNCs to the chemical potential of vapor. The universality classes and the characteristics of the models are studied by the scaling ansatz of kinetic roughening and by measurements of tilt-dependent currents and height step widths. Through measurements of the ratio of number of growth processes at NNCs to those at the chosen column, the key processes which are relevant to the determination of the universality class are also studied. [S1063-651X(99)16410-9]

PACS number(s): 05.40.−a, 05.70.Ln, 68.35.Fx, 81.10.Bk

Recently there has been great interest in surface-roughening phenomena of various growth models because of the possible relevance to physical phenomena such as crystal growths, vapor depositions, etc. [1,2]. In many cases, such surfaces possess a self-affine property. To understand the physical properties of such surfaces, the surface width $W(L,t)$ has been intensively studied. The scaling ansatz for $W(L,t)$ with the linear size of substrate L is

$$W(L,t)=L^{\alpha}f\left(\frac{t}{L^{z}}\right), \tag{1}$$

where the scaling function $f(x)\rightarrow$const for $x\gg 1$, and $f(x)\sim x^{\beta}$ ($\beta=\alpha/z$) for $x\ll 1$ [1–3]. There have been many theoretical efforts to relate various growth models to continuum growth equations [1,2]. One of the most famous growth equations is the Kardar–Parisi–Zhang (KPZ) equation [4]. The models which belong to the KPZ universality class are characterized by nonconserved dynamics [5]. On the other hand, the growth models in which the number of dropped particles to the surfaces is conserved have been studied because of the possible relevance to the molecular-beam-epitaxial (MBE) growths [6–15]. In these conserved models, the main growth processes are depositions and surface relaxations. However, in the real growths, such as chemical vapor depositions (CVDs), and even in MBE growths, there could be evaporation processes [2]. Even though there have been some growth models which consider evaporation processes [12,14,16], there have been few studies that use the real growth models to explain the surface roughenings of the vapor depositions in which the evaporation processes should be as important as the depositions and surface relaxations. The motivation of this paper is, therefore, to establish the more realistic growth models in which the evaporation processes are treated as equal to the depositions and surface relaxations, and to study the critical properties of such growth models.

Now we would like to describe our models in detail. We have constructed our models only in the substrate dimension $d=1$. The generalization to higher dimensions could easily be established. In our model, the chemical potential μ_v of the vapor is preassigned and is never changed during growth. This assumption is believed to describe the thermal equilibrium of the vapor at a certain temperature. We have studied two kinds of models in which the evaporation-deposition processes at the randomly chosen column or at its nearest neighbor columns (NNCs) are determined by the chemical potential differences. The local chemical potential of the surface is defined by local curvature of the surface [9]

$$\mu(x)=-\nabla^2 h(x)=2h(x)-h(x+1)-h(x-1). \tag{2}$$

The first model (*A* model) is defined as what follows [see Fig. 1(a)]. Select a column x randomly and calculate the chemical potentials $\mu(x)$ and $\mu(x\pm1)$ using Eq. (2). Determine the minimum $\mu_{\min}(x')$ and maximum $\mu_{\max}(x'')$ among the $\mu(x)$ and $\mu(x\pm1)$. Here, $x',x''\in\{x,x\pm1\}$. If $\mu_{\max}>\mu_{\min}\geqslant\mu_v$, then decrease the interface height at column x'' as $h(x'')\rightarrow h(x'')-1$ (*evaporation process*). If $\mu_{\min}<\mu_v$, then increase the height at column x' as $h(x')\rightarrow h(x')+1$ (*deposition process*). If $\mu_{\max}=\mu_{\min}=\mu_v$, choose randomly one of the columns among x and $x\pm1$, and do either the deposition or evaporation process randomly at the chosen column.

The second model (*B* model) is defined as follows [see Fig. 1(b)]. Select a column x randomly and calculate the chemical potential $\mu(x)$. If $\mu(x)>\mu_v$, decrease the height at x as $h(x)\rightarrow h(x)-1$ (*evaporation process*). If $\mu(x)<\mu_v$, calculate the chemical potentials $\mu_0=2[h(x)+1]-h(x+1)-h(x-1)$, $\mu_+=2[h(x+1)+1]-h(x+2)-h(x)$, and $\mu_-=2[h(x-1)+1]-h(x-2)-h(x)$. If $\mu(x)<\mu_v$ and μ_0 is the minimum among μ_0 and $\mu_\pm$, then $h(x)\rightarrow h(x)+1$ (*deposition process at the chosen column*). If $\mu(x)<\mu_v$ and $\mu_\pm$ is the minimum among μ_0 and $\mu_\pm$, then $h(x\pm1)\rightarrow h(x\pm1)+1$ (*deposition process at an NNC of the chosen column*). If $[\mu_v=\mu(x)]$, take the random action between deposition and evaporation at x.

The essential difference between the *A* model and the *B* model is the following. In the *A* model, the randomly chosen column and its NNCs are treated equally. Therefore, a particle is evaporated or deposited not only at the randomly

*Electronic address: ykimnms.kyunghee.ac.kr

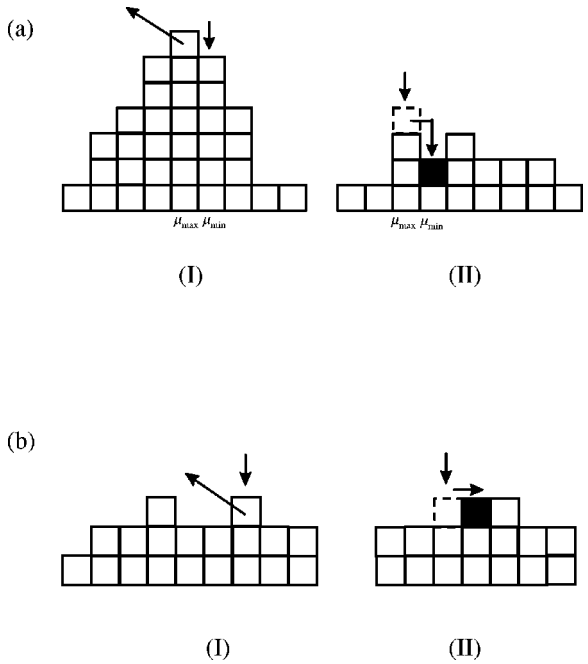

FIG. 1. Possible growth processes in (a) *A* model and (b) *B* model for $\mu_v=1$. $\downarrow$ denotes the randomly selected column, $\nwarrow$ denotes the evaporation site, and dark sites correspond to the growth site. Case (I)'s represent the evaporations and case (II)'s represent depositions at a nearest neighbor column.

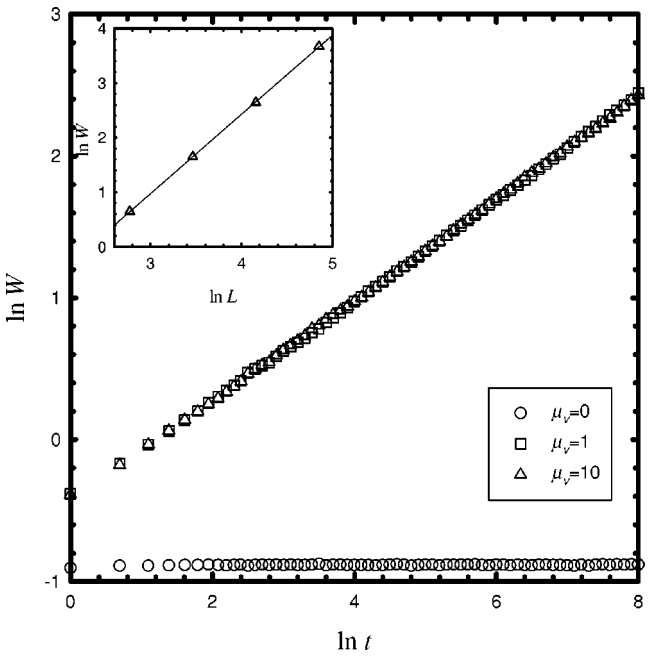

FIG. 2. ln-ln plot of the surface width $[W(L,t)]$ against the Monte Carlo growth time (t) for *A* model for $L=1024$. Inset shows $W(L,\infty)$'s for $L=16,32,64,128$. For $\mu_v>0$, the obtained exponents from the data are $\beta\approx0.37$ and $\alpha\approx1.45$.

chosen column but at NNC. If an NNC is chosen for deposition, then the growth process is essentially the same as the surface relaxations in the Wolf–Villain (WV) model [9] and the Lai–Das Sarma (LD) model [17]. Whereas in the *B* model, the growth process occurring at an NNC is only deposition, and deposition at the NNC is determined by the chemical potential differences between the chosen column and the NNC. The growth processes at NNCs in the *B* model is also the same as the surface relaxations in the Wolf–Villain (WV) model [9] and the Lai–Das Sarma (LD) model [17].

These growth models are expected to follow the equation

$$\frac{\partial h}{\partial t}=\mathcal{F}\{\nabla^2 h(\mathbf{x},t)\}+\eta(\mathbf{x},t), \tag{3}$$

where $\mathcal{F}$ is the local deposition current and is expected to be a functional of the surface curvature $\nabla^2 h(\mathbf{x},t)$. The possible form for $\mathcal{F}$ is

$$\mathcal{F}\{\nabla^2 h\}=\nu_2\nabla^2 h-\nu_4\nabla^4 h + (\textit{nonlinear terms of } \nabla^2 h+\cdots). \tag{4}$$

The critical properties of the suggested models have been studied through the various simulations. In our simulations, we have used periodic boundary conditions and started with the flat substrate $[h(x)=0]$. All results have been averaged over 100 independent runs. First, we will discuss the simulation results for the *A* model. Figure 2 shows the measured $W(L,t)$'s for the *A* model on the substrate size $L=1024$. For $\mu_v=0$, we can see that *W* saturates immediately after starting the growth. In contrast, we have obtained $\beta=0.37\pm0.01$ for $\mu_v>0$ from the data shown in Fig. 2 and the relation $W\sim t^{\beta}$. For the case of $\mu_v=0$, the local chemical potential of the initial substrate is in equilibrium with the chemical potential of the vapor. So there should be no room for making the surface rough. But for $\mu_v>0$, the interface should become rough to reach the equilibrium with the vapor. The inset of Fig. 2 shows the dependence of $W(L,t=\infty)$ on L for $L=16,32,64,128$ when $\mu_v=10$. From the relation $W\sim L^{\alpha}$, we obtained $\alpha=1.45\pm0.01$. These values of β and α with $\mu_v>0$ are close to $\beta=3/8$, $\alpha=3/2$, which are the exact values for the surface roughenings described by the Mullins–Herring (MH) equation [8], i.e., Eq. (3) with $\nu_4>0$, $\nu_2=0$, and $(\cdots)=0$. Villain has introduced a similar model with evaporation processes [14]. In the Villain model a particle can be evaporated or deposited only at a randomly chosen column and there are no growth processes at NNCs. The surface development in the Villain model is well-known to follow the Edwards–Wilkinson (EW) equation [6], i.e., Eq. (3) with $\nu_2>0$, $\nu_4=0$ and $(\cdots)=0$, regardless of the value of μ_v. In contrast, the equal treatment of the randomly chosen column and its NNCs in the *A* model can make the effective surface relaxations [see Fig. 1(a)]. Such effective surface relaxations ensure that the *A* models belong to the MH universality class if $\mu_v>0$.

Now let us discuss the simulation results for the *B* model. In Fig. 3, the initial behavior of $W(L,t)$ as a function of time t on the substrate size $L=1024$ is displayed. From the data for $\mu_v=0$ and 1, we obtained $\beta=0.24\pm0.01$. This value is very close to $\beta=1/4$ for the EW equation. But the data for $\mu_v=10$ give $\beta=0.37\pm0.01$. Inset (a) of Fig. 3 shows the measured β's of the *B* model as a function of μ_v. As shown in the inset, β increases rapidly from $\beta=0.24$ and saturates to $\beta=0.37$ around $\mu_v=3$. Inset (b) of Fig. 3 shows $W(L,t=\infty)$'s. From the data for $\mu_v=0$, we obtained $\alpha=0.49\pm0.01$ (dashed line), and from the data for $\mu_v=10$ we ob-

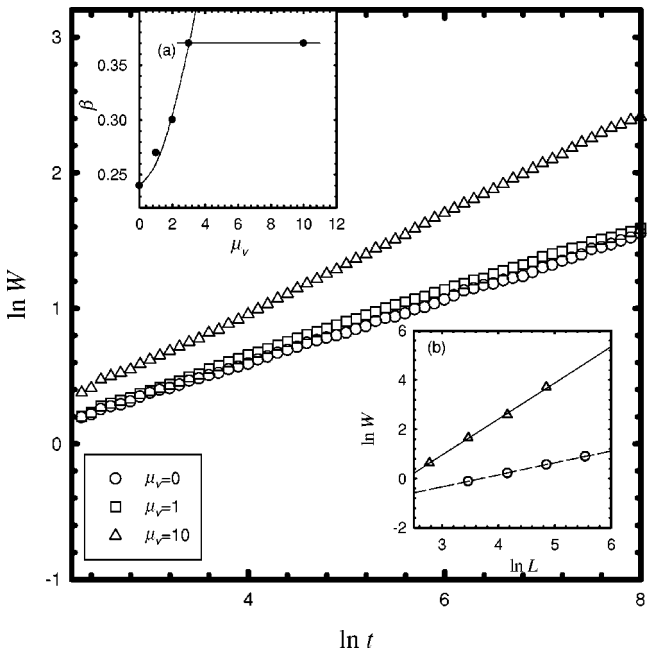

FIG. 3. ln-ln plot of the surface width $[W(L,t)]$ against the Monte Carlo growth time (t) for the B model for $L=1024$. Inset (a) shows the plot of obtained β's against μ_v. Inset (b) shows $W(L,\infty)$'s for $\mu_v=0$ and for $\mu_v=10$. The obtained exponents are $\beta\approx 0.24$ for $\mu_v=0,1$ and $\beta\approx 0.37$ for $\mu_v=10$. Obtained α's from the data in inset (b) are $\alpha\approx 0.49$ for $\mu_v=0$ and $\alpha\approx 1.47$ for $\mu_v=10$, respectively.

tained $\alpha=1.47\pm 0.01$ (solid line). These results also imply that the B models with lower values of μ_v belong to the EW universality class, whereas those with higher values of μ_v $(\mu_v>3)$ seem to belong to the MH universality class.

The EW term in the Villain model should be from the evaporation-deposition processes [14] at the chosen column. Since our models also have the evaporation-deposition processes at the chosen column, it is natural to suspect a slow crossover to the EW universality class as in the WV model [9,10]. In order to test the existence of the similar crossover, we have used the method suggested by Krug *et al.* [18]. The coefficient ν_2 in Eq. (4) can be determined by the tilt-dependent current $J(m)$ through the relation [18]

$$\nu_2=-\left.\frac{\partial J(m)}{\partial m}\right|_{m=0}, \tag{5}$$

where m is the average slope of the substrate. If our models have the EW term with $\nu_2(>0)$, then there must be negative tilt-dependent current as in the WV model [18]. We measured each $J(m)$ by taking 6.4×10^8 processes on the substrate size $L=1024$. We have found no meaningful negative $J(m)$'s in the A model. This result supports the assertion that the A model belongs to the MH universality class regardless of the μ_v value if $\mu_v>0$. The measured data of $J(m)$ for the B model are displayed in Fig. 4. As shown in Fig. 4, for small $\mu_v(=2,3)$ we have found the negative currents [18] which depend on the slope m. From the data in Fig. 4 and Eq. (5) we obtained $\nu_2\approx 0.4$ for $\mu_v=2$ and $\nu_2\approx 0.1$ for $\mu_v=3$. But the measured $J(m)$'s for $\mu_v>3$ did not seem to show clear negative values and did not clearly show any tilt

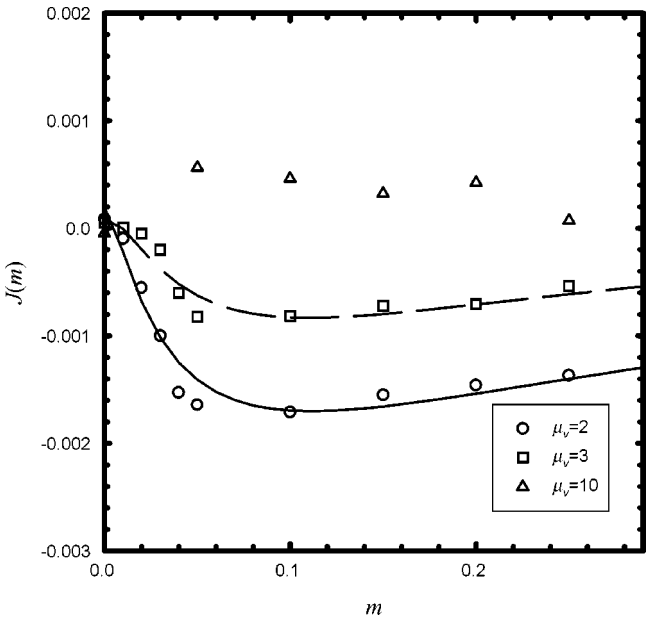

FIG. 4. Plot of $J(m)$ against m for B models. The measured negative currents for $\mu_v=2,3$ indicate that $\nu_2\neq 0$ [see Eq. (5)]. The data for $\mu_v=10$ show no tilt-dependent negative current.

dependency. These results support the assertion that the B models with $\mu_v\leqslant 3$ belong to the EW universality class and seem to support the assertion that those with $\mu_v>3$ belong to the MH universality class. More recently, a useful scaling relation for the height step width [19]

$$G(1,t;L)\equiv\langle[h(x,t)-h(x+1,t)]^2\rangle \tag{6}$$

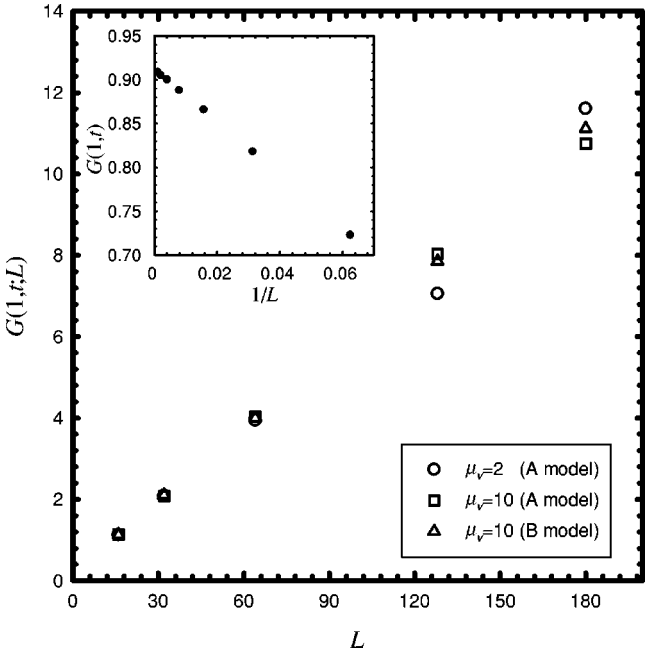

FIG. 5. Plot of $G(1,t;L)$ against L in the steady-state regime. Inset shows the data of the B model with $\mu_v=2$. For the A model, the behavior of $G(1,t;L)$ follows Eq. (8) for both $\mu_v=2$ and $\mu_v=10$. For the B model, the behavior of $G(1,t;L)$ follows Eq. (7) for $\mu_v=2$ and follows Eq. (8) for $\mu_v=10$.

was used to test the existence of the EW term in the WV model. $G(1,t;L)$ is known to scale as

$$G(1,t;L)\sim\begin{cases}\text{const.}-1/L & \text{for } t\gg L^2\\ \text{const.} & \text{for } t\ll L^2,\end{cases} \tag{7}$$

for the models of the EW universality class, and as

$$G(1,t;L)\sim\begin{cases}L & \text{for } t\gg L^4\\ t^{1/4} & \text{for } t\ll L^4,\end{cases} \tag{8}$$

for the models of the MH universality class. As shown in Fig. 5, the data of $G(1,t;L)$ for the A model follow Eq. (8) for both $\mu_v=2$ and $\mu_v=10$. This result also supports the theory that the A model with an arbitrary value of μ_v belongs to the MH universality class. But the data for the B model with $\mu_v=2$ follow Eq. (7) and those with $\mu_v=10$ follow Eq. (8). This result also supports the assertion that model B with small $\mu_v(<3)$ belongs to the EW universality class, but model B with $\mu_v(>3)$ seems to belong to the MH universality class. Even though measurements of the tilt-dependent currents and height step widths suggested the absence of the EW term in model B with larger μ_v, the suggestion has come from the simulations on finite-sized substrates. As long as the evaporation is possible only at the chosen site, an EW term as well as a MH term should exist in the B model for all values of μ_v. In the simulation on the finite-sized substrates, it could therefore be possible that the EW term may become less important than the MH term if μ_v is increased. However, in the strict long time and in the large L limit, there could exist no transition between the MH and EW universality classes in the B model regardless of μ_v value.

Now we would like to discuss the key processes which discriminate the models that belong to the EW universality class from those that belong to the MH universality class. If the growth processes at the chosen column are more effective than the growth processes at NNCs (the effective surface relaxations) [14], the growth of interface should follow the EW equation. In contrast, if the growth processes at NNCs are more dominant than those at the chosen column, then the growth model should belong to the MH universality class [2]. To see these theoretical expectations clearly in our models, we measured the ratio $R(\mu_v)$ of the number of the growth processes at NNCs occurring in the steady-state regime to those of the evaporation-deposition processes at the chosen site. The ratio $R(\mu_v)$ can be defined as

$$R(\mu_v)=\frac{[\text{number of growth processes at NNCs}]}{[\text{number of deposition and evaporation processes at the chosen column}]}. \tag{9}$$

We measured $R(\mu_v)$ from 6.4×10^8 processes on the substrate size $L=1024$. As shown in Fig. 6, measured $R(\mu_v)$'s for the A models do not change as μ_v (>0) is varied. The measured $R(\mu_v)$'s of model A indicate that the number of growth processes at NNCs is much greater than that of evaporation-deposition processes at the chosen column and the $R(\mu_v)$ hardly changes if $\mu_v(>0)$ is varied. These results support that the growth processes at NNCs are more dominant than the evaporation-deposition processes at the chosen column. This fact is the essential origin for A models with $\mu_v(>0)$ that belong to the MH universality class. In the B model, the measured $R(\mu_v)$ shows somewhat complex behavior. The value of $R(\mu_v)$ increases as μ_v increases when $\mu_v\leqslant3$. In this range of μ_v, the evaporation-deposition processes at the chosen column are still effective, and these effective evaporation-deposition processes make B models with $\mu_v<3$ belong to the EW universality class. However, for $\mu_v>3$, $R(\mu_v)$ saturates to nearly the same value as that of the A model and do not change as μ_v increases. So, for $\mu_v>3$, the growth processes at NNCs become more effective and the B models seem to belong to the MH universality class.

In summary, we have studied two models for vapor depositions in which evaporation-deposition processes can occur both at a randomly chosen column and at its NNCs. The measurements of surface width, tilt-dependent current, and height step width for the A model have shown that A models for $\mu_v>0$ belong to the MH universality class. In contrast, B models have been shown to belong to the MH universality class for $\mu_v>3$, and B models with $\mu_v\leqslant3$ have been shown to belong to the EW universality class. The measurements of $R(\mu_v)$ for both A and B models have shown good agreement with the conclusions drawn from measurements of β's.

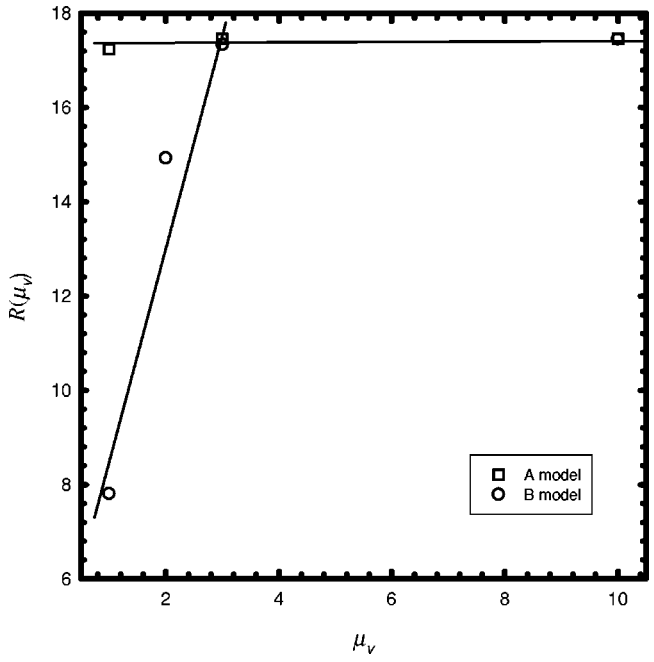

FIG. 6. Plot of $R(\mu_v)$ against the μ_v in the steady-state regime. For the definition of $R(\mu_v)$ see Eq. (9).

From these results we can conclude the following facts. If the growth processes at NNCs are more dominant than the evaporation-deposition processes at the chosen column, then the corresponding models belong to the MH universality class. In contrast, if the evaporation-deposition processes at the chosen column are effective, then the corresponding models belong to the EW universality class.

This work was supported in part by the Korean Science and Engineering Foundation (Grant No. 98-07-02-05-01-3).

[1] F. Family and T. Vicsek, *Dynamics of Fractal Surfaces* (World Scientific, Singapore, 1991); J. Krug and H. Sphon, in *Solids Far From Equilibrium: Growth, Morphology and Defects*, edited by C. Godreche (Cambridge University Press, New York, 1991).

[2] S. V. Barabási and H. E. Stanley, *Fractal Concepts in Surface Growth* (Cambridge University Press, New York, 1995).

[3] F. Family and T. Vicsek, J. Phys. A: Math. Gen. **18**, L75 (1985).

[4] M. Kardar, G. Parisi, and Y.-C. Zhang, Phys. Rev. Lett. **56**, 889 (1986).

[5] M. J. Void, J. Colloid Interface Sci. **18**, 684 (1963); D. N. Sutherland, *ibid.* **22**, 300 (1966); R. Baoid, D. Kessler, P. Rammanlal, L. M. Sander, and R. Savit, Phys. Rev. A **38**, 3672 (1988); F. Jullien and R. Botet, J. Phys. A: Math. Gen. **18**, 2279 (1985); J. Kertész and D. E. Wolf, *ibid.* **21**, 747 (1988); J. M. Kim and J. M. Kosterlitz, Phys. Rev. Lett. **62**, 2289 (1989).

[6] S. F. Edwards and D. R. Wilkinson, Proc. R. Soc. London, Ser. A **381**, 17 (1982).

[7] F. Family, J. Phys. A: Math. Gen. **19**, L441 (1986).

[8] C. Herring, J. Appl. Phys. **21**, 301 (1950); W. W. Mullins, *ibid.* **28**, 333 (1957); **30**, 77 (1959).

[9] D. E. Wolf and J. Villain, Europhys. Lett. **13**, 389 (1990).

[10] P. Šmilauer and M. Kotrla, Phys. Rev. B **49**, 5769 (1994); M. Kotrla and P. Šmilauer, *ibid.* **53**, 13 777 (1996).

[11] S. Das Sarma and P. Tamborenea, Phys. Rev. Lett. **66**, 325 (1991).

[12] J. M. Kim and S. Das Sarma, Phys. Rev. E **48**, 2599 (1993).

[13] J. M. Kim and S. Das Sarma, Phys. Rev. Lett. **72**, 2903 (1994).

[14] J. Villain, J. Phys. I **1**, 19 (1991).

[15] Yup Kim, D. K. Park, and J. M. Kim, J. Phys. A: Math. Gen. **27**, L553 (1994); S. H. Yook, J. M. Kim, and Yup Kim, Phys. Rev. E **56**, 4085 (1997).

[16] D. D. Vvedensky, A. Zangwill, C. N. Luse, and M. R. Wilby, Phys. Rev. E **48**, 852 (1993).

[17] Z.-W. Lai and S. Das Sarma, Phys. Rev. Lett. **66**, 2348 (1991).

[18] J. Krug, M. Plischke, and M. Siegert, Phys. Rev. Lett. **70**, 3271 (1993).

[19] K. Park, B. Kahng, and S. S. Kim, Physica A **210**, 146 (1994).